A&A 386, 134–139 (2002)
DOI: 10.1051/0004-6361:20020216

Astronomy & Astrophysics

Hα surface photometry of galaxies in the Virgo cluster III. Observations with INT and NOT 2.5 m telescopes⋆,⋆⋆

A. Boselli[1], J. Iglesias-Páramo[1], J. M. Vílchez[2], and G. Gavazzi[3]

[1] Laboratoire d'Astronomie Spatiale, Traverse du Siphon, 13376 Marseille Cedex 12, France
e-mail: Alessandro.Boselli@astrsp-mrs.fr,Jorge.Iglesias@astrsp-mrs.fr
[2] Instituto de Astrofísica de Andalucía (CSIC), Apdo. 3004, 18080, Granada, Spain
e-mail: jvm@iaa.es
[3] Università degli Studi di Milano-Bicocca, Piazza delle scienze 3, 20126 Milano, Italy

Received 3 December 2001 / Accepted 5 February 2002

Abstract. We present Hα line imaging observations of 30 galaxies obtained at the 2.5 m INT and NOT telescopes. The observed galaxies are mostly BCD Virgo cluster galaxies. Hα+[NII] fluxes and equivalent widths, as well as images of all the detected targets are presented. With these observations, Hα data are available for ≃50% of the BCD galaxies listed in the VCC.

Key words. galaxies: photometry – galaxies: fundamental parameters

1. Introduction

This paper is the third of a series devoted to Hα+[NII] imaging observations of Virgo cluster galaxies: in Gavazzi et al. (2002; Paper I), we present Hα imaging data obtained with the 2.1 m of San Pedro Martir, mostly of low luminosity spirals and irregulars. In Boselli & Gavazzi (2002; Paper II) we present data obtained with the 1.2 m telescopes at the Observatoire de Haute Provence and at Calar Alto for the brightest galaxies in the cluster. This paper presents Hα imaging data obtained at the 2.5 m INT and NOT telescopes for blue compact dwarfs (BCDs) galaxies in Virgo. These data are aimed at completing the Hα survey of BCD galaxies of Almoznino et al. (1998) and Heller et al. (1999) aimed at studying the star formation activity in low-mass, dwarf galaxies. These objects are particulary useful to test whether the scaling relations of giant spirals, as derived by Boselli et al. (2001), hold true at the low end of the luminosity function. Given the lack of spiral patterns in BCDs, star formation cannot be triggered by compression from gravitational density waves and rotational shear, as in giant spirals, but is probably governed by random collision of interstellar clouds (Hunter et al. 1998). These characteristics make BCDs and dwarf irregulars a unique class of objects for studying the physical conditions behind the star formation.

Data for other bright galaxies, serendipitously observed in the Wide Field Camera (WFC) at the INT are also presented.

The analysis based on these data will be discussed in future communications.

2. The sample

Galaxies observed in this work have been selected from the Virgo Cluster Catalogue (VCC) of Binggeli et al. (1985), which is complete to the optical B magnitude $m_{\rm pg} = 18.0$. We selected all BCD galaxies (BCD, Im/BCD, Sm/BCD) classified as cluster members, possible members or belonging to the W, W', M clouds or to the southern extension (Binggeli et al. 1985, 1993).

Among the 67 BCD Virgo cluster members matching these criteria, 34 objects (51%) either included in the present work or in Paper I have an Hα measurement. If limited to the ISO sample described in Boselli et al. (1997), 16 out 18 BCD galaxies (89%) have Hα data.

Given the large field of view of the WFC at the INT, some galaxies not matching the selection criteria were serendipitously observed in the fields of other targets.

Send offprint requests to: A. Boselli,
e-mail: Giuseppe.Gavazzi@mib.infn.it

⋆ Based on observations taken at the INT and NOT telescopes, operated on the island of La Palma by the ING and NOT teams in the Spanish Observatorio del Roque de Los Muchachos of the Instituto de Astrofsica de Canarias.

⋆⋆ Figure 1 is only available in electronic form at http://www.edpsciences.org

Table 1. The target galaxies.

VCC (1)	NGC/IC (2)	UGC (3)	RA(1950) (4)	Dec (5)	a (6)	b (7)	Vel (8)	Clust (9)	Dist (10)	θ (11)	Type (12)	m_{pg} (13)	B_T^0 (14)	H_T (15)
24	-	-	120 802.5	120 220.0	1.00	0.37	1289	M	32	4.99	BCD	14.95	15.79	12.68
144	-	-	121 245.0	60 220.0	0.63	0.32	2014	W	32	7.66	BCD	15.31	15.18	12.95
213	3094	7305	121 423.4	135 413.0	0.93	0.71	–162	N	17	3.60	dS/BCD	14.26	14.74	11.52
324	-	7354	121 636.5	40 758.0	1.35	1.15	1524	S	17	9.01	BCD	14.78	14.30	11.83
404	-	7387	121 743.8	42 844.0	1.71	0.21	1733	S	17	8.60	Scd	15.00	13.90	-
428	-	-	121 807.9	140 959.0	0.39	0.11	794	A	17	2.89	BCD	17.50	-	-
459	-	-	121 839.6	175 457.0	0.84	0.36	2108	A	17	5.74	BCD	14.95	-	12.72
513	-	-	121 924.0	23 718.0	0.73	0.61	1832	S	17	10.28	BCD	15.10	-	12.33
655	4344	7468	122 105.8	174 906.0	1.55	1.55	1147	A	17	5.44	Spec/BCD	13.21	13.58	10.66
787	4376	7498	122 245.1	60 104.0	1.84	1.07	1136	B	23	6.79	Scd	13.69	13.38	11.08
793	-	-	122 249.8	132 060.0	0.47	0.34	1906	A	17	1.50	Im	16.74	17.26	14.85
802	-	-	122 257.0	134 624.0	0.64	0.21	–215	A	17	1.71	BCD	17.40	17.61	14.64
810	-	-	122 301.8	133 006.0	0.77	0.77	–340	A	17	1.53	dE	16.95	17.06	14.04
815	-	-	122 305.4	132 512.0	0.66	0.53	–700	A	17	1.47	dE	16.10	16.59	-
846	-	-	122 318.0	132 818.0	0.89	0.80	–730	A	17	1.46	dE	16.20	16.58	-
848	-	-	122 319.8	60 506.0	1.16	0.98	1537	B	23	6.70	Im/BCD	14.72	15.18	13.35
873	4402	7528	122 335.3	132 320.0	3.95	1.16	234	A	17	1.36	Sc	12.56	11.74	8.58
1297	-	-	122 800.0	124 600.0	0.51	0.45	1486	A	17	0.12	E	14.33	14.42	10.25
1313	-	-	122 816.6	121 916.0	0.45	0.20	1254	A	17	0.35	BCD	17.15	17.30	15.60
1316	4486	7654	122 817.6	124 002.0	11.00	11.00	1292	A	17	0.00	E	9.58	9.82	6.21
1369	-	-	122 901.2	122 024.0	0.50	0.20	1022	A	17	0.37	dE	17.30	-	-
1437	-	-	123 001.2	92 658.0	0.59	0.45	1160	S	17	3.25	BCD	15.12	-	12.21
1488	3487	-	123 041.4	94 030.0	1.26	0.53	1157	S	17	3.05	E	14.76	-	-
1725	-	-	123 509.4	85 001.0	1.55	0.97	1068	S	17	4.19	Sm/BCD	14.51	14.61	12.13
1804	-	-	123 708.4	94 024.0	0.75	0.20	1898	E	17	3.70	Im/BCD	15.63	16.30	13.31
1955	4641	7889	124 036.5	121 928.0	1.36	1.07	2012	E	17	3.02	Spec/BCD	14.32	-	11.16
2007	3716	-	124 215.6	82 254.0	0.78	0.41	1857	E	17	5.49	Im/BCD	15.20	-	13.33
2033	-	-	124 333.0	84 454.0	0.73	0.73	1486	E	17	5.42	BCD	14.65	15.60	13.06
2034	-	-	124 336.6	102 612.0	0.78	0.52	1500	E	17	4.36	Im	15.82	16.24	13.23
2037	-	-	124 343.8	102 848.0	0.88	0.38	1142	E	17	4.37	Im/BCD	15.92	16.20	12.55
2045	-	-	124 424.0	102 724.0	1.29	0.43	-	E	17	4.52	dE	16.33	-	-

The target galaxies, as well as the serendipitously observed objects, are listed in Table 1, arranged as follow:

- Column 1: VCC designation, from Binggeli et al. (1985);
- Column 2: NGC or IC name;
- Column 3: UGC name (Nilson 1973);
- Columns 4 and 5: (B1950.0) celestial coordinates, from NED;
- Columns 6 and 7: major an minor optical diameters measured on the du Pont plates at the faintest detectable isophote;
- Column 8: heliocentric velocity, in $\mathrm{km\,s^{-1}}$, from the VCC;
- Column 9: cluster membership as defined in Gavazzi et al. (1999);
- Column 10: distance, in Mpc. Distances to the various substructures of Virgo are as given in Gavazzi et al. (1999);
- Column 11: angular distance from the cluster centre, in degrees;
- Column 12: morphological type as given in the VCC;
- Column 13: photographic magnitude from the VCC;
- Column 14: optical magnitude determined and corrected for dust extinction as described in Gavazzi & Boselli (1996);
- Column 15: total extrapolated H band magnitude, uncorrected for extinction, determined as described in Gavazzi et al. (2000a). For galaxies observed in the K band (Boselli et al. 1997), H magnitudes are determined using the observed colour index $H-K$ when available, or assuming an average $H-K=0.25$.

3. Observations

Narrow band imaging in the Hα emission line (λ = 6562.8 Å) of galaxies was obtained in 1999 at the 2.5 m INT and in 2000 and 2001 at the 2.56 m NOT telescope at El Roque de los Muchachos, La Palma, Canary Islands. The INT observations were carried out with the Wide Field Camera (WFC) attached at the prime focus of the telescope. The WFC is composed by a science array of four thinned AR coated EEV 4 K×2 K CCDs, plus a fifth acting as autoguider. The pixel scale at the detectors is 0.33 arcsec pixel^{-1}, which gives a total field of view of about 34×34 arcmin^2. Given the particular arrangement of the detectors, a squared area of about 11×11 arcmin^2 is lost at the top right corner of the field. The top left corner of detector #3 is also lost because of vignetting of the filters.

The $f/11$ 2.56 m NOT telescope is equipped with a Loral/Lesser 2048×2048 pixel CCD detector. The pixel size is 0.19 arcsec. At the adopted gain, the electron/adu conversion is 1 e^-/adu, with a readout noise of 6 e^-. A total of 4 nights at the INT and 6 at NOT were allocated to this project. Of these, 5.5 were totally or partly useful due to technical problems or weather limitations, as reported in Table 2 (logbook of the observations and CCD technical data). One galaxy (VCC 24) was observed at the INT in service mode.

Each galaxy was observed through one narrow band interferometric filter (see Table 3) centered at the redshifted Hα line (ON), while the red continuum near Hα (OFF) was generally taken in a broad band filter. The filters given

Table 2. Logbook of the observations.

Telescope	Date	Nights (ass./used)	CCD	Pixel size
2.5 m INT	17–20/2/1999	4/3.5	WFC	0.333
2.56 m NOT	29/4–1/5/2000	3/0.5	Loral/Lesser 2048 × 2048	0.188
2.56 m NOT	27–29/4/2001	3/1.5	Loral/Lesser 2048 × 2048	0.188

in Table 3 are used as ON or OFF band for each target as specified in Cols. 2 and 3 of Table 4. The flux from the [NII] emission lines at $\lambda 6548$ Å and $\lambda 6584$ Å is included in the ON band observations. The typical integration time was of 3×1800–1500 min ON- and 3×600–200 min OFF-band for the INT observations, and 3×1500–900 min ON- and 3×300–900 min for the broad and narrow OFF-band observations at the NOT. NOT observations were obtained during good seeing conditions (∼1 arcsec), fairly good at the INT (1.5–2 arcsec).

The observations were calibrated using the standard stars Feige 56, 66, 67 and BD 33+2642 from the catalogue of Massey et al. (1988) or from the IRAF compilation. Observations of the standard stars were repeated every 2 hours, with an integration time of 3–30 s. At least once per night a calibration star was observed on each CCD of the WFC to allow cross calibration of the different chips. The zero point of each galaxy is determined assuming an extinction law of slope 0.06 for the 1999 run, 0.1 for the other runs. Repeated measurements gave <10% differences, which we assume as the typical uncertainty of the photometry given in this work. All frames except one were obtained in photometric conditions. The determination of the Hα equivalent width can however be achieved also in non photometric conditions using field stars to normalize the ON and OFF band images, as described in Paper I.

4. Image analysis

The data reduction of the CCD images follows a procedure identical to the one described in previous papers of this series (Gavazzi et al. 1998; Papers I and II), based on IRAF/ STSDAS[1] data reduction packages. To remove the detector response each image is bias subtracted and divided by the mean of several flat field exposures obtained on the twilight sky. In some cases images were fitted with a 2-D polynomial function to remove second order structures in the image. A median combination of the realigned images allows removal of cosmic rays. Subtraction of contaminating objects, such as nearby stars and galaxies, is done by direct editing of the frames. The sky background is determined in each frame in concentric object-free annuli around the object. The typical uncertainty on the mean background is estimated 10% of the rms in the individual pixels. This represents the dominant source of error in low S/N regions.

[1] IRAF is the Image Analysis and Reduction Facility made available to the astronomical community by the National Optical Astronomy Observatories, which are operated by AURA, Inc., under contract with the U.S. National Science Foundation. STSDAS is distributed by the Space Telescope Science Institute, which is operated by the Association of Universities for Research in Astronomy (AURA), Inc., under NASA contract NAS 5–26555.

Table 3. The characteristics of the adopted filters

Filter	λ	$\Delta\lambda$	$R(\lambda)$	$\int R(\lambda)\mathrm{d}\lambda$	Telescope
6568	6574	95	89	83.95	INT
R	6380	1520	83	1307.73	INT
6562	6562	33	66	24.68	NOT
6564	6564	46	74	39.18	NOT
6610	6610	50	76	43.74	NOT
6883	6883	65	77	50.50	NOT
r	6800	1020	86	1249.41	NOT

Total counts in the two frames have been obtained by integrating the pixel counts over the area covered by each galaxy, as derived by the optical major and minor diameters. Fluxes and equivalent widths and errors are computed using Eqs. (1) and (2) and (6) and (7) of Paper I, assuming $K = 1$.

We corrected for the contamination of the Hα+[NII] line emission in the broad band filter (OFF-band) using the following relations:

$$F(\mathrm{H}\alpha + [\mathrm{NII}])_\mathrm{c} = F(\mathrm{H}\alpha + [\mathrm{NII}])_\mathrm{o} \left(1 + \frac{\int R_\mathrm{ON}(\lambda)\mathrm{d}\lambda}{\int R_\mathrm{OFF}(\lambda)\mathrm{d}\lambda}\right) \quad (1)$$

and

$$\mathrm{H}\alpha + [\mathrm{NII}]EW_\mathrm{c} = \mathrm{H}\alpha + [\mathrm{NII}]EW_\mathrm{o} \left(1 + \frac{\mathrm{H}\alpha + [\mathrm{NII}]EW_\mathrm{o}}{\int R_\mathrm{OFF}}\right) \times \left(1 + \frac{\int R_\mathrm{ON}(\lambda)\mathrm{d}\lambda}{\int R_\mathrm{OFF}(\lambda)\mathrm{d}\lambda}\right) \quad (2)$$

where $F(\mathrm{H}\alpha+[\mathrm{NII}])_\mathrm{o}$ and $\mathrm{H}\alpha+[\mathrm{NII}]EW_\mathrm{o}$ are the observed values (from Eqs. (1) and (2) in Paper I), $F(\mathrm{H}\alpha + [\mathrm{NII}])_\mathrm{c}$ and $\mathrm{H}\alpha+[\mathrm{NII}]EW_\mathrm{c}$ the corrected ones and R_ON and R_OFF the trasmissivity of the filters given in Col. 4 of Table 3.

5. Results

The results of the present observations are listed in Table 4, arranged as follow:

- Column 1: galaxy name;
- Column 2 and 3: ON and OFF band filters;
- Column 4: telescope used;

Table 4. The results of the observations.

									This work					Literature			
VCC	ON	OFF	Tel	Year	T_{ON}	T_{OFF}	R(Ha)	$n_{\frac{ON}{OFF}}$	Hα + [NII]EW	F(Hα + [NII])	Phot	Morph	Notes	Hα + [NII]EW	F(Hα + [NII])	Ref.	Notes
(1)	(2)	(3)	(4)	(5)	(6)	(7)	(8)	(9)	(10)	(11)	(12)	(13)	(14)	(15)	(16)	(17)	
24	6568	r	INT	2001	33	10	0.86	0.30	3 ± 1	-14.03 ± 0.04	C	C		-1	-	A	*
144	6610	r	NOT	2001	45	15	0.75	0.18	161 ± 1	-12.23 ± 0.04	P	C		159 ± 22	-12.72	A	
213	6564	r	NOT	2000	40	10	0.61	0.13	24 ± 2	-12.67 ± 0.05	P	El					
324	6568	R	INT	1999	75	25	0.85	0.20	65 ± 8	-12.29 ± 0.06	P	C		56 ± 4	-12.20	A	*
404	6568	R	INT	1999	75	25	0.83	0.21	8 ± 1	-13.22 ± 0.07	P	D					
428	6562	r	NOT	2000	60	30	0.53	0.09	251 ± 19	-12.97 ± 0.04	P	C					
459	6610	r	NOT	2001	45	15	0.75	0.19	48 ± 1	-12.66 ± 0.04	P	E		56 ± 7	-12.53	A	*
513	6610	r	NOT	2001	45	15	0.73	0.19	49 ± 1	-12.72 ± 0.04	P	C		53 ± 5	-12.66	A	
655	6568	R	INT	1999	77	18	0.87	0.23	7 ± 1	-12.75 ± 0.07	P	El		3 ± 1		Hi	*
787	6568	R	INT	1999	47	10	0.87	0.46	22 ± 1	-12.48 ± 0.04	P	C+E					
793	6568	R	INT	1999	75	20	0.73	0.23	$- \pm 4$	-	P						
802	6568	R	INT	1999	75	20	0.86	0.24	38 ± 4	-13.54 ± 0.06	P	E					
810	6568	R	INT	1999	75	20	0.85	0.23	-1 ± 6	-	P						
815	6568	R	INT	1999	75	20	0.84	0.23	-1 ± 7	-	P						
846	6568	R	INT	1999	75	20	0.84	0.23	-1 ± 5	-	P						
848	6568	R	INT	1999	47	10	0.83	0.47	28 ± 5	-13.02 ± 0.08	P	E		14		GS	
873	6568	R	INT	1999	75	20	0.88	0.23	12 ± 1	-12.09 ± 0.05	P	D		10 ± 2	-12.18	II	*
1297	6568	R	INT	1999	75	5	0.85	1.00	-1 ± 1	-	P						
1313	6568	R	INT	1999	75	25	0.86	0.20	351 ± 10	-12.84 ± 0.04	P	C					
1316	6568	R	INT	1999	75	5	0.86	1.00	2 ± 3	-12.05 ± 0.63	P	FIL		1 ± 3	-11.73	M	*
1369	6568	R	INT	1999	75	25	0.87	0.20	-1 ± 8	-	P						
1437	6568	R	INT	1999	90	23	0.87	0.20	17 ± 2	-13.16 ± 0.07	P	C					
1488	6568	R	INT	1999	90	23	0.87	0.20	-1 ± 3	-	P		*				
1725	6568	R	INT	1999	75	7	0.87	0.25	43 ± 9	-12.66 ± 0.08	P	C+E		38 ± 5	-12.62	A	*
1804	6610	6883	NOT	2001	60	45	0.73	1.47	3 ± 1	-14.37 ± 0.19	P	D					
1955	6610	r	NOT	2000	20	5	0.74	0.25	9 ± 4	-13.10 ± 0.17	P	C					
2007	6610	6883	NOT	2001	60	45	0.73	1.45	10 ± 1	-13.77 ± 0.04	P	E					
2033	6568	R	INT	1999	75	25	0.85	0.22	13 ± 3	-13.32 ± 0.10	P	C		5 ± 3	-13.68	A	*
2034	6568	R	INT	1999	75	10	0.85	0.50	2 ± 2	-14.29 ± 0.44	P	L		2 ± 1	-13.81	H	*
2037	6568	R	INT	1999	75	10	0.87	0.50	17 ± 6	-13.51 ± 0.16	P	C		16 ± 1		Hi	
2045	6568	R	INT	1999	75	10	0.87	0.50	-1 ± 4	-	P		*				

Notes: long slit spectra were taken by Gavazzi et al., in prep., for VCC 24 (Hα + [NII]EW = 19 Å), VCC 324 (Hα + [NII]EW = 313 Å), VCC 459 (Hα + [NII]EW = 67 Å), VCC 655 (Hα + [NII]EW = 22 Å), VCC 873 (Hα + [NII]EW = 14 Å), VCC 1725 (Hα + [NII]EW = 77 Å) and VCC 2033 (Hα + [NII]EW = 33 Å).
VCC 1316: our Hα data are already discussed in Gavazzi et al. (2000b).
VCC 1488: possible vignetting.
VCC 2034: the flux might be contaminated by a nearby bright star.
VCC 2045: no redshift available; assumed at the average velocity of the cluster, vel = 1200 km s^{-1}
References:
A: Almoznino & Brosch (1998); H: Heller et al. (1999); Hi: Hippelein et al. in prep; M: Macchetto et al. (1996); II: Paper II. GS: Gavazzi et al., in preparation (spectroscopic survey drifting the telescope over the entire disc of the galaxy).

– Column 5: year of the observation;
– Column 6: total integration time ON band;
– Column 7: total integration time OFF band;
– Column 8: transmissivity of the filter at the given redshifted Hα line;
– Column 9: normalization factor obtained by dividing the flux of several field stars in the ON band frame to the OFF band frame, $n_{\frac{\rm ON}{\rm OFF}}$. In photometric conditions this quantity gives the transmission difference between the ON and the OFF band filters. Under non photometric conditions $n_{\frac{\rm ON}{\rm OFF}}$ includes variations in the sky transparency. The average values $n_{\frac{\rm ON}{\rm OFF}}$ obtained in photometric conditions are $n_{\frac{6568}{R}} = 0.067 \pm 0.003$ for the INT, $n_{\frac{6610}{r}} = 0.062 \pm 0.002$ and $n_{\frac{6610}{6883}} = 1.095 \pm 0.016$ for the NOT;
– Column 10: Hα+[NII] equivalent width (Hα + [NII]EW), and error, in Å;
– Column 11: log of the Hα+[NII] flux and error, in erg cm^{-2} sec^{-1}, uncorrected for underlying Balmer absorption and galactic extinction;
– Column 12: a flag indicates whether the frame was taken under photometric (P) or cirrus (C) conditions;
– Column 13: Hα+[NII] morphology of the galaxy, as in Brosch et al. (1998): C indicates a giant, central starburst region, E emission from the edge of the galaxy, El emission along a ring structure, D diffuse emission, L linear (HII regions along the disc) and FIL a filamentary structure;
– Column 14: notes to the present observations;
– Columns 15 and 16: Hα + [NII]EW and F(Hα + [NII]) flux from the literature;
– Column 17: references to the Hα data available in the literature;
– Column 18: notes to the reference data.

The red continuum images of all the observed galaxies are shown as contours plots superposed to the Hα+[NII] net image (grey levels) in Fig. 1. In most BCD galaxies (53% of the targets) the Hα emission is dominated by a central sturburst region, as in VCC 1313, or by giant HII regions at the edges of the disc, as in VCC 459 (24%). In few objects, such as VCC 655, the emission is along a ring-like structure, or it is diffuse and/or homogeneously distributed along the disc (VCC 2034).

5.1. Comparison with the literature

Fluxes and equivalent widths given in this paper are in general consistent with available measurements, as shown in Fig. 2. The average value of the difference between our measurements and those in the literature is: Hα + [NII]$EW_{\rm TW}$ − Hα + [NII]$EW_{\rm L}$ = 1.9 ± 4.5 Å and − log F(Hα + [NII])$_{\rm TW}$ + log F(Hα + [NII])$_{\rm L}$ = 0.02 ± 0.29 erg cm^{-2} s^{-1}. This has been estimated excluding long-slit spectroscopic data from (Gavazzi et al. in prep.), which, in the case of BCD, could be non-representative of the whole galaxy but biased towards high surface brightness HII regions, as in the case of VCC 24, 324, 655 and 2033. The significant difference between our Hα+[NII] flux estimate and that of Heller et al. (1999) for VCC 2034 might be due to the contamination by a nearby star.

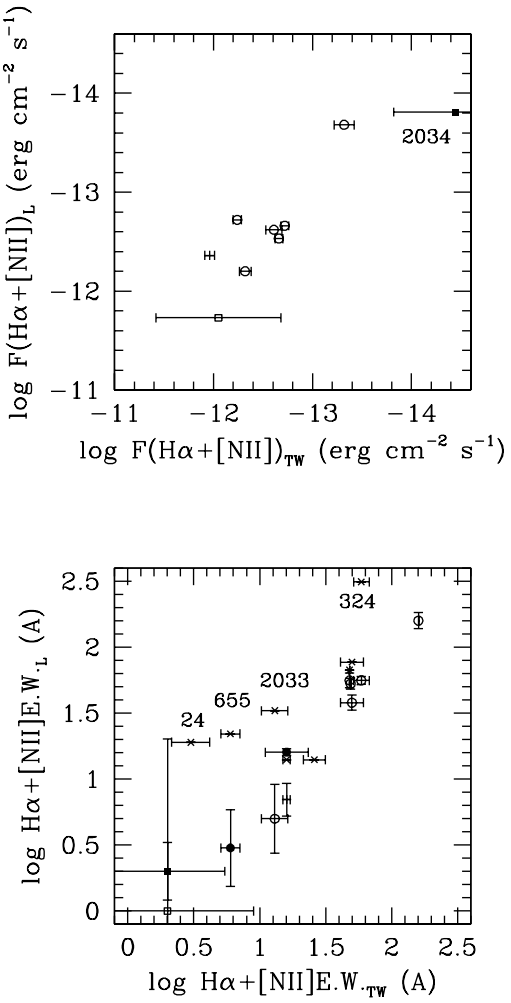

Fig. 2. Comparison with data in the literature: open dots are for A, filled dots for Hi, open squares for M, filled squares for H, + for I and X for G (see Table 4).

6. Summary and conclusion

We present Hα+[NII] imaging data (fluxes and equivalent widths) of 30 Virgo galaxies obtained at the 2.5 m INT and at the 2.56 m NOT telescopes at El Roque de los Muchachos, La Palma. The present observations of BCD galaxies in the Virgo cluster are aimed at completing at low luminosity a large project of multifrequency observations of galaxies spanning a large range in morphological type and luminosity and belonging to different environments (cluster-isolated) for the purpose of constructing a large data-set suitable for statistical studies.

Acknowledgements. We wish to thank the night operators for their assistance during the observations. This project is partly financed by the French PNG. The data presented here have been taken using ALFOSC, which is owned by the Instituto de Astrofisica de Andalucia (IAA) and operated at the Nordic

Optical Telescope under agreement between IAA and the NBIfAFG of the Astronomical Observatory of Copenhagen. We thank L. Cortese for helping us in cros-calibrating photometric observations with spectroscopic data.

References

Almoznino, E., & Brosch, N. 1998, MNRAS, 298, 920
Binggeli, B., Sandage, A., & Tammann, G. 1985, AJ, 90, 1681 (VCC)
Binggeli, B., Popescu, C., & Tammann, G. 1993, A&AS, 98, 275
Boselli, A., Tuffs, R., Gavazzi, G., Hippelein, H., & Pierini, D. 1997, A&A, 121, 507
Boselli, A., & Gavazzi, G. 2002, A&A, 386, 124 (Paper II)
Brosch, N., Heller, A., & Almoznino, E. 1998, MNRAS, 300, 1091
Gavazzi, G., & Boselli, A. 1996, Astro. Lett. and Communications, 35, 1
Gavazzi, G., Boselli, A., Scodeggio, M., Pierini, D., & Belsole, E. 1999, MNRAS, 304, 595
Gavazzi, G., Franzetti, P., Scodeggio, M., Boselli, A., & Pierini, D. 2000a, A&A, 361, 863
Gavazzi, G., Boselli, A., Vilchez, J. M., Iglesias-Paramo, J., & Bonfanti, C. 2000b, A&A, 361, 1
Gavazzi, G., Boselli, A., Pedotti, P., Gallazzi, A., & Carrasco, L. 2002, A&A, 386, 114 (Paper I)
Heller, A., Almoznino, E., & Brosch, N. 1999, MNRAS, 304, 8
Hunter, D., Elmegreen, B., & Baker, A. 1998, ApJ, 493, 595
Kennicutt, R. 1998, ARA&A, 36, 189
Macchetto, F., Pastoriza, M., Caon, N., et al. 1996, A&AS, 120, 463
Massey, P., Strobel, K., Barnes, J., & Anderson, E. 1988, ApJ, 328, 315
Nilson, P. 1973, Uppsala General Catalogue of Galaxies, Uppsala Obs. Ann., vol. 6 (UGC)
Young, C., & Currie, M. 1998, A&AS, 127, 367